Numerical model of a compressible multi-fluid fluctuating flow

Christophe Berthon[†⋆]
Christophe.Berthon@math.u-bordeaux1.fr

Boniface Nkonga[†⋆]
Boniface.Nkonga@math.u-bordeaux1.fr

[†] *MAB UMR 5466 CNRS, Université Bordeaux I, 351 cours de la libération, 33400 Talence, France.*

[⋆] *INRIA Futurs, projet ScAlApplix, Domaine de Voluceau-Rocquencourt, B.P. 105, 78153 Le Chesnay Cedex France.*

Abstract

In the present work, we consider the numerical approximations of multi-fluid compressible fluctuating flows. Assuming that the flow is composed by non mixing compressible fluids, we derived a modelization that can be view as an extension of the standard compressible (k, ϵ). This model is fundamentally in non conservation form (the coupling between fluids and turbulence involves non conservative products) and the usual finite volume methods fail. The nonlinear projection scheme is used to preserve, at the discrete level, the main properties of the model. The numerical computations are performed on the Richtmeyer-Meshkov instability to validate the approach and to measure the influence of fluctuations.

Key words : compressible flows, velocity fluctuations, non-conservative equations, nonlinear projection methods

1 Introduction

When modeling non mixing multi-fluid flow, one generally assume that, at a given point of the domain, only one component is present. Therefore, averaged variables are always associated to an unique component of the fluid. This ideal situation is well posed when the different interfaces are explicitly characterized and tracked. Based on this observation, some numerical methods have been developed [7, 9, 10,

12, 13, 14, 21, 26]. The main difficulties in these approach are the computations of interfaces/interfaces and interfaces/waves interactions. The problem becomes crucial when there are many complex interfaces.

The numerical approach proposed in this paper does not explicitly characterize or track the interfaces. Interfaces are approximated by a set of characteristic volumes where the fluid components are supposed mixed. The physics in these volumes has to be defined in order to be able to reproduce coherent interfaces/interfaces and interfaces/waves interactions. Therefore, we consider a set of equations, derived from an ensemble averaging [11], describing the behavior of a multi-component flow. The number of variables in these modelizations grows with the number of flow components [23]. This model is well posed in general, but turns out to be efficient only for flows with few components. Based on the assumption that pressure and velocity relaxations are instantaneous, some simplified models have been developed [1, 24, 18, 25]. In these cases, the effects of velocity fluctuations are not considered.

The regime investigated in this paper is non mixed flow, at the physical model level and weakly mixed flow, at the numerical model level. In this context, some assumptions are introduced to derived a simplify well posed model containing all the main characteristics of the flow as the residual viscous effects. One of the main assumption is that, locally, all the components of the fluid have the same average velocity. However, the modelization takes into account the difference between the average velocity and the velocity of each components. Therefore, the modelization takes into account the velocity fluctuations and, under the Boussinesq approximation, the problem is well posed. Moreover, some entropy balance equations are obtained and they are still valid at the vanishing viscosity limit.

Numerical method is developed, in the finite volumes framework. The physical model used in the present work is governed by non-conservative equations and some non classical behaviors have to be considered [8, 22]. At the discrete level these properties are preserved by a nonlinear projection formulation [2, 3]. Sources terms are split and integrated analytically. The proposed numerical approach is validated with the computation of the Richtmeyer-Meshkov interface instability.

The paper is organized as follows. In the first section the derivation of physical model is proposed and the mathematical properties are established. The second section is devoted with the numerical approximation. Then, numerical results are presented and analyzed before the conclusion.

2 The physical model

Let us consider a multi-component flow and assume that heat effects, body forces and some dissipation terms can be neglected. Using ensemble averaging, Drew and Passman [11] derived the following model for multi-component flow [11](pages 126-130):

$$\partial_t(\alpha_\ell\tilde{\rho}_\ell) + \nabla\cdot(\alpha_\ell\tilde{\rho}_\ell\mathbf{u}_\ell) = \dot{\tilde{\rho}}_\ell, \tag{1}$$

$$\partial_t(\alpha_\ell\tilde{\rho}_\ell\mathbf{u}_\ell) + \nabla\cdot(\alpha_\ell\tilde{\rho}_\ell\mathbf{u}_\ell\otimes\mathbf{u}_\ell) = \nabla\cdot(\alpha_\ell(\sigma_\ell+\sigma'_\ell)) + \dot{\mathbf{u}}_\ell, \tag{2}$$

$$\partial_t(\alpha_\ell\tilde{\rho}_\ell\mathrm{e}_\ell) + \nabla\cdot(\alpha_\ell\tilde{\rho}_\ell\mathrm{e}_\ell\mathbf{u}_\ell) = \alpha_\ell\sigma_\ell:\nabla\mathbf{u}_\ell + \alpha_\ell\tilde{\rho}_\ell\epsilon_\ell + \dot{\mathrm{e}}_\ell \tag{3}$$

and

$$\alpha_\ell \tilde{\rho}_\ell \epsilon_\ell = -\partial_t(\alpha_\ell \tilde{\rho}_\ell k_\ell) - \nabla \cdot (\alpha_\ell \tilde{\rho}_\ell k_\ell \mathbf{u}_\ell) + \alpha_\ell \sigma'_\ell : \nabla \mathbf{u}_\ell + \dot{k}_\ell, \tag{4}$$

where α_ℓ, $\tilde{\rho}_\ell$, $\mathbf{u}_\ell$, e_ℓ and σ_ℓ are respectively the averaged volume fraction, density, velocity, internal energy and stress tensor of the fluid component. The kinetic turbulent energy of fluid components is denoted k_ℓ while ϵ_ℓ denotes its dissipation rate. The mean density $\tilde{\rho}_\ell$ is the mass of constituent ℓ per unit volume of constituent ℓ. The notation $\tilde{\rho}_\ell$ must not be confused with ρ_ℓ that denotes the partial density (also called the effective density of the component ℓ).

The production of mass $\dot{\tilde{\rho}}_\ell$, momentum $\dot{\mathbf{u}}_\ell$, total energy $\dot{\mathrm{e}}_\ell$, and kinetic turbulent energy $\dot{k}_\ell$ are defined by the transfer at the interfaces. Du to conservation properties, we have:

$$\sum_\ell \dot{\tilde{\rho}}_\ell = \sum_\ell \dot{\mathbf{u}}_\ell = \sum_\ell \dot{\mathrm{e}}_\ell = \sum_\ell \dot{k}_\ell = 0 \tag{5}$$

When there is no phase transition or chemical reaction at interfaces we have $\dot{\tilde{\rho}}_\ell = 0$. These equations are obtained by introducing a fluctuation velocity which is the difference $\mathbf{u}'_\ell$ between the complete field $\mathbf{v}$ and the mean field $\mathbf{u}_\ell$ in a representative volume:

$$\mathbf{u}'_\ell = \mathbf{v} - \mathbf{u}_\ell, \tag{6}$$

where $\mathbf{u}_\ell$ is constant in the representative volume of the averaging approach. The fluctuation $\mathbf{u}'_\ell$ is defined only where the fluid component ℓ is present. Then, the Reynolds stress σ'_ℓ and the fluctuation kinetic energy k_ℓ are associated to $\mathbf{u}'_\ell$.

In order to derived a simplify model, we assume that relaxation processes are instantaneous, such that the averaged velocity is the same for all components:

$$\mathbf{u}_\ell = \mathbf{u} \quad \text{for all } \ell. \tag{7}$$

Therefore

$$\mathbf{u}'_\ell = \mathbf{u}', \quad k_\ell = k, \quad \epsilon_\ell = \epsilon \quad \text{for all } \ell. \tag{8}$$

The mean stress tensors are defined by $\sigma_\ell = -p_\ell Id + \mu_\ell \tau(\mathbf{u})$. Therefore, under the Boussinesq approximation, the Reynolds stress is put under the form:

$$\sigma'_\ell = -p'_\ell Id + \mu'_\ell \tau(\mathbf{u}) \quad \text{with} \quad p'_\ell = (\gamma' - 1)\tilde{\rho}_\ell k \tag{9}$$

where p'_ℓ is the spherical part of the tensor, γ' is a constant ($\gamma' = \frac{5}{3}$ for frictionless collisions [11]) and μ'_ℓ is the coefficient of fluctuation viscosity. After [3] (see also [6]), we adopt the notation γ', instead of 5/3, which makes more practical several computations (for instance, see the lemma 2.2).

Summing over all components the mass, the momentum and the fluctuation kinetic energy, we obtain:

$$\partial_t \rho + \nabla \cdot (\rho \mathbf{u}) = 0, \tag{10}$$

$$\partial_t(\rho \mathbf{u}) + \nabla \cdot (\rho \mathbf{u} \otimes \mathbf{u}) + \nabla(p + p') = \nabla \cdot ((\mu + \mu')\tau(\mathbf{u})), \tag{11}$$

$$\partial_t(\rho k) + \nabla \cdot (\rho k \mathbf{u}) + p' \nabla \cdot (\mathbf{u}) = \mu' \tau(\mathbf{u}) : \nabla \mathbf{u} - \rho \epsilon, \tag{12}$$

where

$$\rho = \sum_\ell \alpha_\ell \tilde{\rho}_\ell, \quad p = \sum_\ell \alpha_\ell p_\ell, \quad p' = \sum_\ell \alpha_\ell p'_\ell, \tag{13}$$

$$\mu = \sum_\ell \alpha_\ell \mu_\ell, \quad \mu' = \sum_\ell \alpha_\ell \mu'_\ell.$$

As in the turbulence modelization, the evolution of the dissipation rate $\rho\epsilon$ is approximated as follows:

$$\partial_t(\rho\epsilon) + \nabla\cdot(\rho\epsilon\mathbf{u}) + \frac{2}{3}C_1\rho\epsilon\nabla\cdot(\mathbf{u}) = \mu^{''}\tau(\mathbf{u}) : \nabla\mathbf{u} - R \tag{14}$$

where

$$\mu^{''} = C_1\frac{\epsilon}{k}\mu', \quad R = C_2\rho\frac{\epsilon^2}{k}$$

where C_1 and C_2 are modeling constants. When the fluctuations are at the turbulence level, some numerical values of these constants can be found in [19]. In a representative volume of the model the components are isolated (even in a micro-scale description [11](page 100)). Therefore, the mass fraction Y_ℓ, the volume fraction α_ℓ, the mean density $\tilde{\rho}_\ell$ and the partial density ρ_ℓ are related by the following relations:

$$Y_\ell = \frac{m_\ell}{m} = \frac{\tilde{\rho}_\ell V_\ell}{\rho V} = \frac{\tilde{\rho}_\ell}{\rho}\alpha_\ell \Longrightarrow \rho_\ell = \rho Y_\ell = \tilde{\rho}_\ell\alpha_\ell \tag{15}$$

m and V are notations for mass and volume. We assume that the relaxation processes are instantaneous (the same mean velocity) and that there is no phase transition or chemical reactions. Therefore, we have $\dot{\mathrm{e}}_\ell = 0$ and the balance of internal energy of each component writes as:

$$\partial_t(\rho_\ell \mathrm{e}_\ell) + \nabla\cdot(\rho_\ell \mathrm{e}_\ell\mathbf{u}) + \alpha_\ell p_\ell\nabla\cdot(\mathbf{u}) = \alpha_\ell\mu_\ell\tau(\mathbf{u}) : \nabla\mathbf{u} + \rho_\ell\epsilon$$

The derived model is then described by the balance equations:

$$\partial_t\rho + \nabla\cdot(\rho\mathbf{u}) = 0, \tag{16}$$

$$\partial_t(\rho\mathbf{u}) + \nabla\cdot(\rho\mathbf{u}\otimes\mathbf{u}) + \nabla(p+p') = \nabla\cdot\left((\mu+\mu')\tau(\mathbf{u})\right), \tag{17}$$

$$\partial_t(\rho_\ell \mathrm{e}_\ell) + \nabla\cdot(\rho_\ell \mathrm{e}_\ell\mathbf{u}) + \alpha_\ell p_\ell\nabla\cdot(\mathbf{u}) = \alpha_\ell\mu_\ell\tau(\mathbf{u}) : \nabla\mathbf{u} + \rho_\ell\epsilon, \tag{18}$$

$$\partial_t(\rho k) + \nabla\cdot(\rho k\mathbf{u}) + p'\nabla\cdot(\mathbf{u}) = \mu'\tau(\mathbf{u}) : \nabla\mathbf{u} - \rho\epsilon, \tag{19}$$

$$\partial_t(\rho\epsilon) + \nabla\cdot(\rho\epsilon\mathbf{u}) + \frac{2}{3}C_1\rho\epsilon\nabla\cdot(\mathbf{u}) = C_1\tfrac{\epsilon}{k}\mu'\tau(\mathbf{u}) : \nabla\mathbf{u} - C_2\tfrac{\rho\epsilon^2}{k} \tag{20}$$

where $p' = (\gamma' - 1)\rho k$. The model recovers the usual equation for the total energy $E = \frac{1}{2}\rho\mathbf{u}^2 + \rho k + \sum_\ell \rho_\ell \mathrm{e}_\ell$. Indeed, from (18) we deduce

$$\partial_t(\sum_\ell \rho_\ell \mathrm{e}_\ell) + \nabla\cdot\left(\sum_\ell \rho_\ell \mathrm{e}_\ell\mathbf{u}\right) + p\nabla\cdot(\mathbf{u}) = \mu\tau(\mathbf{u}) : \nabla\mathbf{u} + \rho\epsilon. \tag{21}$$

Now, from (17) we compute the evolution law of the kinetic energy. We set

$$\mathbf{u}\cdot\Big(\partial_t(\rho\mathbf{u}) + \nabla\cdot(\rho\mathbf{u}\otimes\mathbf{u}) + \nabla(p+p')\Big) = \mathbf{u}\cdot\Big(\nabla\cdot\big((\mu+\mu')\tau(\mathbf{u})\big)\Big). \tag{22}$$

Since we have

$$\begin{aligned}\mathbf{u}\cdot\partial_t\rho\mathbf{u} &= \rho\partial_t\frac{\mathbf{u}^2}{2}+\mathbf{u}^2\partial_t\rho,\\ &= \partial_t\rho\frac{\mathbf{u}^2}{2}-\mathbf{u}^2\nabla\cdot(\rho\mathbf{u}),\end{aligned}$$

and

$$\mathbf{u}\cdot\nabla\cdot(\rho\mathbf{u}\otimes\mathbf{u})=\nabla\cdot\left(\rho\frac{\mathbf{u}^2}{2}\mathbf{u}\right)+\frac{\mathbf{u}^2}{2}\nabla\cdot(\rho\mathbf{u}),$$

the equation (22) reads as follows:

$$\partial_t\left(\rho\frac{\mathbf{u}^2}{2}\right)+\nabla\cdot\left(\rho\frac{\mathbf{u}^2}{2}\mathbf{u}\right)+\mathbf{u}\nabla(p+p')=\mathbf{u}\cdot\nabla\cdot\big((\mu+\mu')\tau(\mathbf{u})\big). \tag{23}$$

We sum (19), (21) and (23) to obtain

$$\partial_t E+\nabla\cdot\left((E+p+\frac{2}{3}\rho k)\mathbf{u}\right)=\mathbf{u}\cdot\nabla\cdot\big((\mu+\mu')\tau(\mathbf{u})\big)+(\mu+\mu')\tau(\mathbf{u}):\nabla\mathbf{u}.$$

Assume that $\tau(\mathbf{u})$ is symmetric to write

$$\mathbf{u}\cdot\nabla\cdot\big((\mu+\mu')\tau(\mathbf{u})\big)+(\mu+\mu')\tau(\mathbf{u}):\nabla\mathbf{u}=\nabla\cdot\big((\mu+\mu')\tau(\mathbf{u})\mathbf{u}\big).$$

The usual conservation of the total energy is thus obtained:

$$\partial_t E+\nabla\cdot\left((E+p+\frac{2}{3}\rho k)\mathbf{u}\right)=\nabla\cdot\big((\mu+\mu')\tau(\mathbf{u})\mathbf{u}\big) \tag{24}$$

In order to obtain a well posed problem, we need more closure assumptions.

2.1 Closure assumptions and mathematical properties

Let us consider in this section the following 1D formulation of the previous system for a mixture of n_p components:

$$\begin{cases}\partial_t\rho+\partial_x\rho u=0,\\ \partial_t(\rho u)+\partial_x(\rho u^2+p+\frac{2}{3}\rho k)=\partial_x((\mu+\mu')\partial_x u),\\ \partial_t(\rho_\ell e_\ell)+\partial_x(\rho_\ell e_\ell u)+\tilde{p}_\ell\partial_x u=\tilde{\mu}_\ell(\partial_x u)^2+\rho_\ell\epsilon,\quad 1\le\ell\le n_p,\\ \partial_t(\rho k)+\partial_x(\rho k u)+\frac{2}{3}\rho k\partial_x u=\mu'(\partial_x u)^2-\rho\epsilon,\\ \partial_t(\rho\epsilon)+\partial_x(\rho\epsilon u)+\frac{2}{3}C_1\rho\epsilon\partial_x u=C_1\frac{\epsilon}{k}\mu'(\partial_x u)^2-C_2\rho\frac{\epsilon^2}{k},\end{cases} \tag{25}$$

where $\tilde{p}_\ell=\alpha_\ell p_\ell$ and $\tilde{\mu}_\ell=\alpha_\ell\mu_\ell$.

Let us denote by s_ℓ the specific entropy of a given component. The second law of the thermodynamic laws, for each component of the fluid, is written as:

$$de_\ell=-T_\ell ds_\ell-p_\ell dv_\ell, \tag{26}$$

where $T_\ell>0$ is the temperature and v_ℓ is the specific volume. In the present work, s_ℓ is the mathematical entropy instead of $-s_\ell$ which denotes the physical

entropy (see Godlewski and Raviart [15] to further details). As usual, the functions $(v_\ell, s_\ell) \to e_\ell(v_\ell, s_\ell)$ are assumed to be strictly convex and satisfy:

$$\frac{\partial e_\ell}{\partial v_\ell}(v_\ell, s_\ell) = -p_\ell < 0 \quad \text{and} \quad \frac{\partial e_\ell}{\partial s_\ell}(v_\ell, s_\ell) = -T_\ell < 0. \tag{27}$$

According to the modeling assumptions proposed in [16], the thermodynamics are completed by the relations:

$$\left\{ \begin{array}{ll} D_t v_\ell & = \lambda_\ell D_t v \\ D_t \lambda_\ell & = 0 \end{array} \right. \tag{28}$$

where $\lambda_\ell > 0$ is a given set of parameters and $D_t\phi = \partial_t\phi + \mathbf{u}\partial_x\phi$ is the material derivative of the quantity ϕ.

LEMMA 2.1 When the assumptions (28) are considered with $\lambda_\ell = \frac{\rho}{\tilde{\rho}_\ell} = \frac{\alpha_\ell}{Y_\ell}$, smooth solutions of (25)–(28) satisfy the following entropy inequalities:

$$\partial_t \rho s_\ell + \partial_x \rho s_\ell u = -\frac{\lambda_\ell \mu_\ell}{T_\ell}(\partial_x u)^2 - \frac{\rho\epsilon}{T_\ell} \leq 0, \quad \ell = 1,\ n_p. \tag{29}$$

As a consequence, the following entropy balance equations are obtained

$$\frac{\beta_{n_p}}{T_{n_p}}\left\{\partial_t \rho s_\ell + \partial_x \rho s_\ell u\right\} - \frac{\beta_\ell}{T_\ell}\left\{\partial_t \rho s_{n_p} + \partial_x \rho s_{n_p} u\right\} = \frac{\rho\epsilon}{T_\ell T_{n_p}}\left(\beta_\ell - \beta_{n_p}\right), \tag{30}$$

for $1 \leq \ell \leq n_p - 1$, with $\beta_\ell = \dfrac{\lambda_\ell \mu_\ell}{\sum_k \lambda_k \mu_k}$.

Proof. The identity (29) is obtained from the relation:

$$\rho Y_\ell D_t e_\ell + \alpha_\ell p_\ell \partial_x u = \alpha_\ell \mu_\ell (\partial_x u)^2 + \rho_\ell \epsilon.$$

Using (27) and (15), this relation writes as:

$$-\rho Y_\ell p_\ell D_t v_\ell - \rho Y_\ell T_\ell D_t s_\ell + \lambda_\ell Y_\ell p_\ell \partial_x u = \lambda_\ell Y_\ell \mu_\ell (\partial_x u)^2 + \rho_\ell \epsilon.$$

By the assumptions, we have $D_t v_\ell = \lambda_\ell D_t(1/\rho) = \frac{\lambda_\ell}{\rho}\partial_x u$. Therefore

$$-\rho Y_\ell T_\ell D_t s_\ell = \lambda_\ell Y_\ell \mu_\ell (\partial_x u)^2 + \rho Y_\ell \epsilon.$$

Then, (29) is proved and (30) follows. □

The entropy balance equations, we have established in the above result, are devoted to each fluid. In fact, a similar result holds true concerning the turbulence [3, 6]. Indeed, we have:

LEMMA 2.2 The smooth solutions of (25)–(28) satisfy the following turbulent entropy relation

$$\partial_t \rho s' + \partial_x \rho s' u = \frac{\gamma' - 1}{\rho^{\gamma'-1}}\Big(\mu'(\partial_x u)^2 - \rho\epsilon\Big) \quad \text{with} \quad s' = \frac{(\gamma' - 1)\rho k}{\rho^{\gamma'}} \tag{31}$$

As a consequence, the following entropy balance equations are obtained:

$$\mu'\frac{\gamma'-1}{\rho^{\gamma'-1}}\left\{\partial_t\rho s_{n_p}+\partial_x\rho s_{n_p}u\right\}-\frac{\lambda_{n_p}\mu_{n_p}}{T_{n_p}}\left\{\partial_t\rho s'+\partial_x\rho s'u\right\}= \frac{\rho\epsilon}{T_{n_p}}\frac{\gamma'-1}{\rho^{\gamma'-1}}(\mu'-\lambda_{n_p}\mu_{n_p}). \quad (32)$$

Proof. To obtain the identity (31), let us rewrite the evolution law of ρk as follows:

$$\frac{(\gamma'-1)}{\rho^{\gamma'}}\left(\partial_t(\rho k)+u\partial_x(\rho k)+\gamma'\rho k\partial_x u\right)=\frac{(\gamma'-1)}{\rho^{\gamma'}}\left(\mu'(\partial_x u)^2-\rho\epsilon\right). \quad (33)$$

Now, from the continuity law, we have:

$$(\gamma'-1)\rho k\left(\partial_t\frac{1}{\rho^{\gamma'}}+u\partial_x\frac{1}{\rho^{\gamma'}}-\frac{\gamma'}{\rho^{\gamma'}}\partial_x u\right)=0. \quad (34)$$

Then, (33) and (34) give

$$\partial_t s'+u\partial_x s'=\frac{\gamma'-1}{\rho^{\gamma'}}\Big(\mu'(\partial_x u)^2-\rho\epsilon\Big).$$

Using the relation $\rho\Big(\partial_t s'+u\partial_x s'\Big)=\partial_t\rho s'+\partial_x\rho s'u$, the relation (31) is obtained. The equation (32) is obtained by combining (29) and (31). □

From the system (25), it is very easy to derive the following equation:

$$\partial_t\frac{k^{C_1}}{\epsilon}+u\partial_x\frac{k^{C_1}}{\epsilon}=(C_2-C_1)k^{C_1-1}. \quad (35)$$

In the sequel, the variable $\frac{k^{C_1}}{\epsilon}$ will be used instead of $\rho\epsilon$.

To summarize, the energy and the entropy balance equations (see Lemma 2.1), but also the additional turbulent evolution laws (see Lemma 2.2), are used to reformulate the non conservative system (25) under the following equivalent form:

$$\begin{cases}\partial_t\rho+\partial_x\rho u=0,\\ \partial_t\rho u+\partial_x(\rho u^2+p+\frac{2}{3}\rho k)=\partial_x((\mu+\mu')\partial_x u),\\ \partial_t E+\partial_x(E+p+\frac{2}{3}\rho k)u=\partial_x((\mu+\mu')u\partial_x u),\\ \frac{\beta_{n_p}}{T_{n_p}}\left\{\partial_t\rho s_\ell+\partial_x\rho s_\ell u\right\}-\frac{\beta_\ell}{T_\ell}\left\{\partial_t\rho s_{n_p}+\partial_x\rho s_{n_p}u\right\}=\frac{\rho\epsilon}{T_\ell T_{n_p}}(\beta_\ell-\beta_{n_p}),\\ \frac{\lambda_{n_p}\mu_{n_p}}{T_{n_p}}\left\{\partial_t\rho s'+\partial_x\rho s'u\right\}-\mu'\frac{\gamma'-1}{\rho^{\gamma'-1}}\left\{\partial_t\rho s_{n_p}+\partial_x\rho s_{n_p}u\right\}=\\ \qquad\qquad\qquad\qquad\qquad\qquad\qquad\qquad\frac{\rho\epsilon}{T_{n_p}}\frac{\gamma'-1}{\rho^{\gamma'-1}}(\lambda_{n_p}\mu_{n_p}-\mu'),\\ \partial_t\rho\frac{k^{C_1}}{\epsilon}+\partial_x\rho\frac{k^{C_1}}{\epsilon}u=(C_2-C_1)\rho k^{C_1-1},\end{cases} \quad (36)$$

with $1\leq\ell\leq n_p-1$. According to the entropy balance equation, let us just emphasize that s_{n_p} is not an unknown of (36) but turns out to be a function of the unknowns: $s_{n_p}:=s_{n_p}(\rho,\rho u,E,\rho s_1,...,\rho s_{n_p-1},\rho s',\rho k^{C_1}\epsilon)$.

Let us assume here that the viscosity functions are a product of the characteristic viscosity of the phase by a function of the partial temperature. We consider the following arbitrary choice:

$$\lambda_{n_p}\mu_\ell = (Y_\ell T_\ell)^{m_\ell}\bar{\mu}_\ell \quad 1 \le \ell \le n_p,$$

where $m_\ell > 0$ are real constants to be fixed. Then, when the partial temperatures are given ($\tilde{T}_\ell = Y_\ell T_\ell = \tilde{p}_\ell v/(\gamma_\ell - 1)$), the variables β_ℓ can be computed as follows:

$$\beta_\ell = \frac{(\tilde{T}_\ell)^{m_\ell}\bar{\mu}_\ell}{\sum\limits_{1\le l\le n_p}(\tilde{T}_l)^{m_l}\bar{\mu}_l}. \tag{37}$$

Each β_ℓ turns out to be a level set function characterizing material interfaces.

The conservative variable $\mathbf{w}^C$, the associated flux $\mathbf{f}(\mathbf{w})$, the diffusion $D(\mathbf{w})$ and the source S^C terms are defined by:

$$\mathbf{w}^C = \begin{pmatrix} \rho \\ \rho u \\ E \\ \rho Y_1 \\ \frac{\rho k^{C_1}}{\epsilon} \end{pmatrix}, \quad \mathbf{f}(\mathbf{w}) = \begin{pmatrix} \rho u \\ \rho u^2 + p + p' \\ (E + p + p')u \\ \rho Y_1 u \\ \frac{\rho k^{C_1}}{\epsilon} u \end{pmatrix},$$

$$D(\mathbf{w}) = \begin{pmatrix} 0 \\ \partial_x((\mu+\mu')\partial_x u) \\ \partial_x((\mu+\mu')u\partial_x u) \\ 0 \\ 0 \end{pmatrix}, \quad S^C(\mathbf{w}) = \begin{pmatrix} 0 \\ 0 \\ 0 \\ 0 \\ (C_2 - C_1)\rho k^{C_1 - 1} \end{pmatrix},$$

where $\mathbf{w} = {}^t(\mathbf{w}^C, \mathbf{w}^{NC})$. The vector of non conservative variables $\mathbf{w}^{NC}$ and the associated flux $\mathbf{g}(\mathbf{w})$, the source term $S^{NC}(\mathbf{w}, \rho s_{n_p})$ and a vector $Q(\mathbf{w}, \rho s_{n_p})$ are defined by:

$$\mathbf{w}^{NC} = \begin{pmatrix} \rho s_1 \\ \vdots \\ \rho s_{n_p-1} \\ \rho s' \end{pmatrix}, \quad \mathbf{g}(\mathbf{w}) = \begin{pmatrix} \rho s_1 u \\ \vdots \\ \rho s_{n_p-1} u \\ \rho s' u \end{pmatrix},$$

$$Q(\mathbf{w}, \rho s_{n_p}) = \begin{pmatrix} \frac{\beta_1 T_{n_p}}{T_1 \beta_{n_p}} \\ \vdots \\ \frac{\beta_{n_p-1} T_{n_p}}{T_{n_p-1}\beta_{n_p}} \\ \frac{\mu' T_{n_p}(\gamma'-1)}{\lambda_{n_p}\mu_{n_p}\rho^{\gamma'-1}} \end{pmatrix}, \quad S^{NC}(\mathbf{w}, \rho s_{n_p}) = \begin{pmatrix} \frac{\rho\epsilon(\beta_1 - \beta_{n_p})}{T_1\beta_{n_p}} \\ \vdots \\ \frac{\rho\epsilon(\beta_{n_p-1} - \beta_{n_p})}{T_{n_p-1}\beta_{n_p}} \\ \frac{\rho\epsilon}{\lambda_{n_p}\mu_{n_p}(\lambda_{n_p}\mu_{n_p} - \mu')} \frac{\gamma'-1}{\rho^{\gamma'-1}} \end{pmatrix}.$$

Therefore the model rewrites as:

$$\begin{cases} \partial_t \mathbf{w}^C + \partial_x \mathbf{f}(\mathbf{w}) = D(\mathbf{w}) + S^C(\mathbf{w}), \\ \partial_t \mathbf{w}^{NC} + \partial_x \mathbf{g}(\mathbf{w}) = S^{NC}(\mathbf{w}, \rho s_{n_p}) + Q(\mathbf{w}, \rho s_{n_p}) \left\{ \partial_t \rho s_{n_p} + \partial_x \rho s_{n_p} u \right\}. \end{cases} \tag{38}$$

Let us note that the first order extracted system, given by

$$\left\{ \begin{array}{l} \partial_t \mathbf{w}^C + \partial_x \mathbf{f}(\mathbf{w}) = 0 \\ \partial_t \mathbf{w}^{NC} + \partial_x \mathbf{g}(\mathbf{w}) = Q(\mathbf{w}, \rho s_{n_p}) \left\{ \partial_t \rho s_{n_p} + \partial_x \rho s_{n_p} u \right\}, \end{array} \right.$$

is hyperbolic. The eigenvalues are

$$u \pm c, \quad u, \qquad \text{with} \qquad c^2 = \sqrt{\frac{\gamma p + \gamma' p'}{\rho}}.$$

The eigenvalues $u \pm c$ are one order of multiplicity while the eigenvalue u is $n_p + 3$ order of multiplicity. According to the works [4, 16], one can prove the existence of traveling wave solutions. These solutions are useful to propose a definition of shock wave solutions of the non-conservative hyperbolic system (see [8] or [4, 16]). This is not the purpose of the present work and we focus our attention on the numerical approximate solutions.

3 Numerical approximation

This section is devoted to a nonstandard finite volume method to approximate the solutions of the non-conservative system (38). The principle of this method, called "nonlinear projection method", is described in [3] (see also [6]). For the sake of simplicity, this method is presented in this section in the context of the bi-fluid model. The usual numerical methods are based on a two steps splitting method :

Convection is defined by the system:

$$\left\{ \begin{array}{l} \partial_t \mathbf{w}^C + \partial_x \mathbf{f}(\mathbf{w}) = 0, \\ \partial_t \mathbf{w}^{NC} + \partial_x \mathbf{g}(\mathbf{w}) = Q(\mathbf{w}, \rho s_{n_p}) \left\{ \partial_t \rho s_{n_p} + \partial_x \rho s_{n_p} u \right\}, \\ \mathbf{w}(t = 0, .) = \mathbf{w}^n. \end{array} \right. \tag{39}$$

It is solved by a nonlinear projection method. It is important to note that this nonlinear projection procedure can be applied to any hyperbolic system in the form (39). The principle of this method is based on a two steps splitting technique:

- *Time evolution.* For given $\mathbf{w}^n$, the following conservative system is approximated with $\mathbf{w}^n$ as initial data:

$$\left\{ \begin{array}{c} \partial_t \mathbf{w}^C + \partial_x \mathbf{f}(\mathbf{w}) = 0, \\ \partial_t \mathbf{w}^{NC} + \partial_x \mathbf{g}(\mathbf{w}) = 0, \\ \mathbf{w}(t = 0, .) = \mathbf{w}^n. \end{array} \right. \tag{40}$$

  At the end of this first step, we obtain a prediction, denoted $\mathbf{w}^{n+\frac{1}{3}}$.

- *Nonlinear projection.* In this correction step, the variables $\mathbf{w}^{n+\frac{2}{3}}$ computed in the previous step are preserved and the entropy balance equations are enforced:

$$\left\{ \begin{array}{c} \partial_t \mathbf{w}^C = 0, \\ \partial_t \mathbf{w}^{NC} + \partial_x \mathbf{g}(\mathbf{w}) = Q(\mathbf{w}, \rho s_{n_p}) \left\{ \partial_t \rho s_{n_p} + \partial_x \rho s_{n_p} u \right\}, \\ \mathbf{w}(t=0,.) = \mathbf{w}^{n+\frac{1}{3}}. \end{array} \right.$$

  Let us emphasize that the nonlinear projection procedure enforces the consistency between the non-conservative terms and the numerical approximations. The numerical approximation of the non-conservative products is thus free from the numerical viscosity and the discrete form of the diffusion.

Diffusion and source terms are taken into account by solving the system:

$$\left\{ \begin{array}{l} \partial_t \mathbf{w}^C = D(\mathbf{w}) + S^C(\mathbf{w}), \\ \partial_t \mathbf{w}^{NC} = S^{NC}(\mathbf{w}, \rho s_{n_p}), \\ \mathbf{w}^C(t=0,.) = \mathbf{w}^{n+\frac{2}{3}}, \end{array} \right. \tag{41}$$

where $\mathbf{w}^{n+\frac{2}{3}}$ is the solution after the nonlinear projection. At the end of this step we have computed $\mathbf{w}^{n+1}$.

In the next sections we will give details for the different steps of the numerical approximation.

3.1 Convection step: The 1-D case

In order to solve the system (39), one can use an exact or an approximated Godunov solver [3], a relaxation scheme [6] or any other numerical solver. In the present analysis, the entropy inequalities are obtained in the case of an exact Godunov scheme for a bi-fluid mixture.

We consider a structured mesh in space and time, defined by the cells $I_i = (x_{i-\frac{1}{2}}, x_{i+\frac{1}{2}})$ and the time intervals $[t^n, t^{n+1})$:

$$t^n = n\Delta t \quad \text{and} \quad x_{i+\frac{1}{2}} = (i + \frac{1}{2})\Delta x,$$

where Δt is the time step and Δx the cells length. The approximated solution, at time t^n, will be constant in each cells I_i. We denote by $\mathbf{w}_i^n$ the approximate value at time t^n in cell I_i of the variable $\mathbf{w}$. The numerical solution $\mathbf{w}_h^n(x) = \mathbf{w}_h(x, t^n)$ is then defined by:

$$\mathbf{w}_h^n(x) = \mathbf{w}_i^n \quad \text{when} \quad x \in I_i.$$

Under the CFL like condition:

$$\frac{\Delta t}{\Delta x} \max |\lambda_i(\mathbf{w})| \leq \frac{1}{2}, \tag{42}$$

the solution of the Cauchy problem of the system (40), with the initial data $\mathbf{w}_h^n(x)$, is composed by the solutions of non interacting elementary Riemann problems at

the cells interfaces. Let us denote by $\mathbf{w}_{i+\frac{1}{2}}(\xi)$ the exact solution of the elementary Riemann problem centered at $x_{i+\frac{1}{2}}$:

$$\mathbf{w}_{i+\frac{1}{2}}(\xi) = W\left(\xi, \mathbf{w}_i^n, \mathbf{w}_{i+1}^n\right) \quad \text{with} \quad \xi = \frac{x - x_{i+\frac{1}{2}}}{t - t^n}.$$

The Godunov method is obtained by the projection of the solution composed of elementary Riemann problems on the space of piecewise constant functions on the cells. This is achieved by an averaging over each cell [15]. Let us define the numerical flux by:

$$\phi^{\mathbf{w}}_{i+\frac{1}{2}} = {}^t\left(\mathbf{f}(\mathbf{w}_{i+\frac{1}{2}}(0)), \mathbf{g}(\mathbf{w}_{i+\frac{1}{2}}(0))\right),$$

Then the numerical scheme in the conservative first step is:

$$\mathbf{w}_i^{n+\frac{1}{3}} = \mathbf{w}_i^n - \frac{\Delta t}{\Delta x}\left(\phi^{\mathbf{w}}_{i+\frac{1}{2}} - \phi^{\mathbf{w}}_{i-\frac{1}{2}}\right). \tag{43}$$

The convex entropy of the system (40), $\{\rho s_2\}(\mathbf{w}_i^{n+\frac{1}{3}})$ satisfies a discrete entropy inequality:

$$\{\rho s_2\}(\mathbf{w}_i^{n+\frac{1}{3}}) - (\rho s_2)_i^n + \frac{\Delta t}{\Delta x}\left(\phi^{\rho s_2}_{i+\frac{1}{2}} - \phi^{\rho s_2}_{i-\frac{1}{2}}\right) \leq 0, \tag{44}$$

where

$$\phi^{\rho s_2}_{i+\frac{1}{2}} = \phi^{\rho}_{i+\frac{1}{2}} \tilde{s}_2(\mathbf{w}_{i+\frac{1}{2}}(0)).$$

Moreover, the positiveness of $(e_1)_i^{n+\frac{1}{3}}$ and $(e_2)_i^{n+\frac{1}{3}}$ is ensured as soon as the density $\rho_i^{n+\frac{1}{3}}$ is positive.

In general, the rate of the entropy dissipation associated to ρs_2 is strictly negative. By the Jensen inequality, we have:

$$\{\rho s_2\}(\mathbf{w}_i^{n+\frac{1}{3}}) \leq \frac{1}{\Delta x}\int_{x_{i-1/2}}^{x_{i+1/2}} \{\rho s_2\}(\mathbf{w})(x, t^{n+1})dx. \tag{45}$$

This means that the dissipation of the entropy $\{\rho s_2\}$ is strictly negative. On the other hand, the specific entropies s_1 and s' are simply advected by the flow and therefore, are preserved by the classical (L^2) projection step. At the discrete level, these discrepancy results cause the failure of the entropy balance equations (30) and (32). In the second step, the entropy dissipation is redistribute in order to enforce the balance (30) and (32). Therefore, $(\rho s_1)_i^{n+\frac{2}{3}}$ and $(\rho s')_i^{n+\frac{2}{3}}$ are computed from a

discrete approximation of the entropy balance equations:

$$\frac{\beta_i^{n+\frac{1}{3}}}{(T_2)_i^{n+\frac{1}{3}}}\Big(\{\rho s_1\}(\mathbf{w}_i^{n+\frac{2}{3}}) - (\rho s_1)_i^{n+\frac{1}{3}}\Big) - \frac{1-\beta_i^{n+\frac{1}{3}}}{(T_1)_i^{n+\frac{1}{3}}}\left((\rho s_2)_i^{n+\frac{2}{3}} - (\rho s_2)_i^{n+\frac{1}{3}}\right) = 0, \tag{46}$$

$$\frac{(\lambda_2\mu_2)_i^{n+\frac{1}{3}}}{(T_2)_i^{n+\frac{1}{3}}}\Big(\{\rho s'\}(\mathbf{w}_i^{n+\frac{2}{3}}) - (\rho s')_i^{n+\frac{1}{3}}\Big) - (\mu')_i^{n+\frac{1}{3}}\frac{\gamma'-1}{(\rho_i^{n+\frac{1}{3}})^{\gamma'-1}}\left((\rho s_2)_i^{n+\frac{2}{3}} - (\rho s_2)_i^{n+\frac{1}{3}}\right) = 0, \tag{47}$$

where

$$(\rho s_2)_i^{n+\frac{1}{3}} = (\rho s_2)_i^n - \frac{\Delta t}{\Delta x}\left(\phi_{i+\frac{1}{2}}^{\rho s_2} - \phi_{i-\frac{1}{2}}^{\rho s_2}\right).$$

The above nonlinear problem in the unknown $(\mathbf{w}^{NC})_i^{n+\frac{2}{3}}$ can be shown to admit a unique solution as soon as the approximate Riemann solver involved in the first step obeys discrete entropy inequality for the Lax pair $(\rho s_2, \rho s_2 u)$. This in turn uniquely defines $(\rho s_2)_i^{n+\frac{2}{3}}$ according to:

$$(\rho s_2)_i^{n+\frac{2}{3}} = \{\rho s_2\}\Big(\mathbf{w}_i^{n+\frac{2}{3}}\Big).$$

In addition, we have (see [3] for the proof):

THEOREM 3.1 Let us consider the scheme (43). Under the CFL restriction (42), the following discrete entropy inequalities are satisfied:

$$\{\rho\Psi_\ell(s_\ell)\}(\mathbf{w}_i^{n+\frac{2}{3}}) - (\rho\Psi_\ell(s_\ell))_i^n + \frac{\Delta t}{\Delta x}\Big\{\{\rho\Psi_\ell(s_\ell)u\}_{i+1/2}^n - \{\rho\Psi_\ell(s_\ell)u\}_{i-1/2}^n\Big\} \le 0, \quad \ell = 1,2,$$

for any strictly increasing functions Ψ_ℓ assumed to satisfy the convexity of the maps $\mathbf{w} \to \rho\Psi_1(s_1)$ and $\mathbf{w} \to \rho\Psi_2(s_2(\mathbf{w}))$. The following maximum principles for the specific entropies are met:

$$(s_\ell)_i^{n+\frac{2}{3}} \le \max((s_\ell)_{i-1}^n, (s_\ell)_i^n, (s_\ell)_{i+1}^n), \quad \ell = 1,2. \tag{48}$$

The partial specific internal energies $(e_1)_i^{n+\frac{2}{3}}$ and $(e_2)_i^{n+\frac{2}{3}}$ stay positive as soon as the density $\rho_i^{n+\frac{2}{3}}$ is positive and the maximum principles $0 \le (Y_{1,2})_i^{n+\frac{2}{3}} \le 1$ are satisfied.

For the multidimensional cases, only the *time evolution* step is different from the 1D case. However, the numerical flux is obtained by a extended 1D flux at interfaces between cells.

3.2 Diffusion and source terms

In the present paper, we do not develop the discrete formulation of the diffusive operator and we refer the reader to [5, 19] (and the references therein) where several numerical methods are proposed. Concerning the source terms, we assume that the size of source terms is small compared to dynamic of the flow (governed by the hyperbolic system). Therefore, the numerical approximation is achieved by a splitting technique. The Cauchy problem solved in the additional step is :

$$\left\{\begin{array}{l} \partial_t \rho = 0, \quad \partial_t \rho u = 0, \quad \partial_t \rho Y = 0, \\ \partial_t \rho_\ell e_\ell = \rho_\ell \epsilon, \\ \partial_t \rho k = -\rho \epsilon, \\ \partial_t \rho \epsilon = -C_2 \rho \dfrac{\epsilon^2}{k}. \end{array}\right.$$

This system is integrated analytically with the initial value $\mathbf{w}^{n+\frac{2}{3}}$ to obtain:

$$\left\{\begin{array}{l} \rho^{n+1} = \rho^{n+\frac{2}{3}}, \quad u^{n+1} = u^{n+\frac{2}{3}}, \quad Y^{n+1} = Y^{n+\frac{2}{3}}, \\ k^{n+1} = \left(\dfrac{(k^{n+\frac{2}{3}})^{C_2}}{(C_2-1)\epsilon^{n+\frac{2}{3}}\Delta t + k^{n+\frac{2}{3}}} \right)^{\frac{1}{C_2-1}}, \\ \epsilon^{n+1} = \dfrac{\epsilon^{n+\frac{2}{3}} k^{n+1}}{(C_2-1)\epsilon^{n+\frac{2}{3}}\Delta t + k^{n+\frac{2}{3}}}, \\ e_\ell^{n+1} = e_\ell^{n+\frac{2}{3}} + (k^{n+\frac{2}{3}} - k^{n+1}), \quad 1 \leq \ell \leq n_p. \end{array}\right.$$

Therefore the numerical time step is completely defined.

3.3 The 2-D extension

The multidimensional extension does not involve large difficulties excepted the standard problems meet when approximating Euler or Navier-Stokes equations. The 2-D system is given by

$$\left\{\begin{array}{l} \partial_t \mathbf{w}^C + \partial_x \mathbf{F}_1(\mathbf{w}) + \partial_y \mathbf{F}_2(\mathbf{w}) = D(\mathbf{w}) + S^C(\mathbf{w}), \\ \partial_t \mathbf{w}^{NC} + \nabla \cdot (\mathbf{G}(\mathbf{w})) = S^{NC}(\mathbf{w}, \rho s_{n_p}) + Q(\mathbf{w}, \rho s_{n_p}) \left\{ \partial_t \rho s_{n_p} + \nabla \cdot \left(\rho s_{n_p} \mathbf{u} \right) \right\}, \end{array}\right.$$

where

$$\mathbf{w}^C = \begin{pmatrix} \rho \\ \rho \mathbf{u} \\ E \\ \rho Y_1 \\ \frac{\rho k^{C_1}}{\epsilon} \end{pmatrix}, \quad \mathbf{F}_1(\mathbf{w}) = \begin{pmatrix} \rho u_1 \\ \rho u_1^2 + p + p' \\ \rho u_1 u 1_2 \\ (E + p + p') u_1 \\ \rho Y_1 u_1 \\ \frac{\rho k^{C_1}}{\epsilon} u_1 \end{pmatrix}, \quad \mathbf{F}_2(\mathbf{w}) = \begin{pmatrix} \rho u_2 \\ \rho u_1 u 1_2 \\ \rho u_2^2 + p + p' \\ (E + p + p') u_2 \\ \rho Y_1 u_2 \\ \frac{\rho k^{C_1}}{\epsilon} u_2 \end{pmatrix},$$

and

$$\mathbf{u} = \begin{pmatrix} u_1 \\ u_2 \end{pmatrix}, \quad \mathbf{G}(\mathbf{w}) = \begin{pmatrix} \rho s_1 \mathbf{u} \\ \vdots \\ \rho s_{n_p - 1} \mathbf{u} \\ \rho s' \mathbf{u} \end{pmatrix}.$$

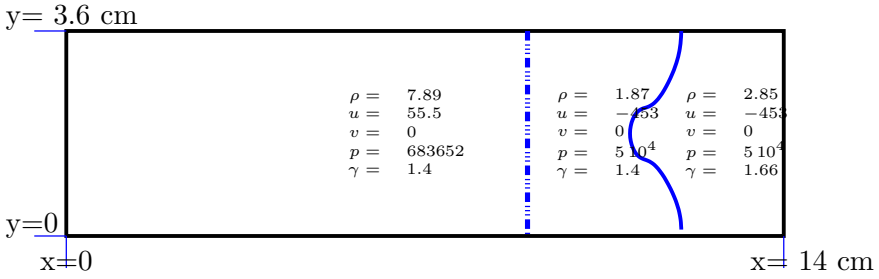

Figure 1: Initialization of the non fluctuating variables.

Once again, we adopt a splitting technique. We do not detail the numerical approximation of the diffusion operator and the source terms which meet a usual form (see [19]). Following the 1-D case, we focus our attention on the convection step.

The updating formula (43) to evolve in time the unknown vector $\mathbf{w}$, is now given by

$$\mathbf{w}_i^{n+\frac{1}{3}} = \mathbf{w}_i^n - \frac{\Delta t}{a_i} \sum_{j \in \mathcal{V}(i)} \phi_{ij}^{\mathbf{w}},$$

where a_i is the area of the control volume, $\mathcal{V}(i)$ denotes the set of the neighboring cells to cell i. The numerical flux function $\phi_{ij}^{\mathbf{w}}$ is computed from the exact or approximate solution of the elementary Riemann problem stated at the cell interface

$$\phi_{ij}^{\mathbf{w}} = \phi^{\mathbf{w}}(\mathbf{n}_{ij}, \mathbf{w}_i^n, \mathbf{w}_j^n),$$

where $\mathbf{n}_{ij}$ is the outer unit normal to the cell interface between cells i and j. The second step of the splitting, namely the nonlinear projection, remains given by (46)-(47) but for the following definition of $(\rho s_2)_i^{n+\frac{1}{3}}$:

$$(\rho s_2)_i^{n+\frac{1}{3}} = (\rho s_2)_i^n - \frac{\Delta t}{a_i} \sum_{j \in \mathcal{V}(i)} \phi_{ij}^{\rho s_2}.$$

The extension of the scheme to multi-dimension is thus achieved.

4 Numerical results

We consider in this section the numerical computation of a 2D Richtmeyer-Meshkov instability. This instability is developed by the interaction of a shock wave with a material interface between two non mixing fluids. We assume that the fluid components are perfect gas and that the fluctuations are at the turbulence scale. Therefore, we can use the following modeling constants: $C_1 = 1.4$ and $C_2 = 1.9$ (see [19]).

The discrete scheme is formulated on unstructured triangular meshes, and the control volumes are of *cell vertex* type (see Nkonga [20]). The numerical fluxes at cells interfaces are computed by the relaxation scheme proposed in [6]. The accuracy of

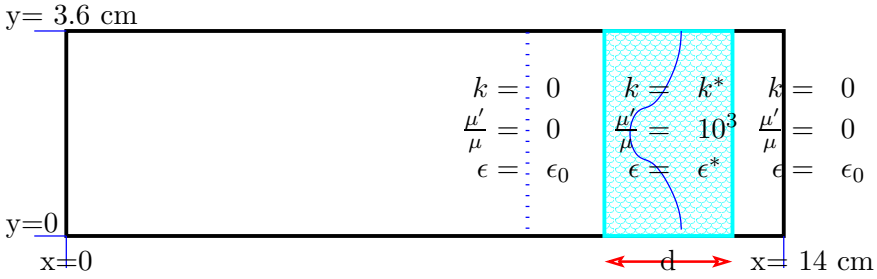

Figure 2: Initialization of the fluctuating variables.

the approximation is improved by a Runge-Kutta second order time approximations and second order space approximations based on a MUSCL type technique.

The computational domain is $[0, 0.14m] \times [0, 0.036m]$ recovered by an unstructured triangulation made of 80000 triangles with 40501 vertices. The characteristic sizes of the mesh are $\Delta x \simeq \frac{0.14}{400}$ and $\Delta y \simeq \frac{0.036}{100}$, the CFL number is fixed to 0.5 for all the computations.

Initially, the two components of the fluid are separated by a oscillating curve interface located at $x = 0.12$ and of size 0.005, defined by (see [16]):

$$x - 0.12 = 0.005 \cos\left(\frac{2\pi(y - 0.018)}{0.036}\right)$$

This interface will be crossed by a shock, initially located at $x = 0.07m$, associated to the left state given by $\rho = 7.89\ kg/m^3$, $P = 683652\ Pa$, $u = 55.5\ m/s$ and the shock wave velocity $\sigma = 213.5\ m/s$. The reader is also referred to the work of Louis [17] where similar numerical experiments are performed.

Computations are performed for different sizes (d) of the fluctuating zone around the interface and for different values of the fluctuating kinetic energy (k^*). The different tests case performed here are defined by:

Test case 0			$d = 0$
Test case A	$k^* = 10\,Pa$	$\epsilon^* = 18$	$d = 5mm$
Test case B	$k^* = 10\,Pa$	$\epsilon^* = 18$	$d = 30mm$
Test case C	$k^* = 30000\,Pa$	$\epsilon^* = 16200000$	$d = 5mm$

The numerical interface is obtained by the fraction β defined by (37). Numerical results give a behavior of the Richtmeyer-Meshkov instability that is accelerated and more developed when fluctuations are considered (figure 4). Indeed, the profile at the time $t = 2.0\ ms$ when there is no fluctuation is comparable to the profile obtained at the time $t = 1.61\ ms$ with an initial fluctuating zone around the material interface (see figure 3). This modification slowly depends on the initial fluctuations zone size or the fluctuation level. The computations obtained for the test cases A, B and C are very close (see figure 5).

5 Conclusion

Under some physical assumptions, we have derived a simplify model for multi-fluid flow, taking into account the influence of velocity fluctuations. The model is close to the classical turbulence model. It is fundamentally non conservative but is associated to some entropy inequalities. Based on the nonlinear projection, we have developed a numerical approximation consistent with the main properties of the model. Numerical computations have point out the importance of the velocity fluctuations on the development of the Richtmeyer-Meshkov instability. Very different behaviors are obtained when fluctuations are considered. However, the global behavior is slowly dependent on the size of the initial fluctuating zone and the level of fluctuations control the velocity of the instabilities.

References

[1] Abgrall R., Nkonga B., and Saurel R., (2003), Efficient numerical approximation of compressible multi-material flow for unstructured meshes. *Computers & Fluids*, 32(4):571–605.

[2] Berthon C., (2002), Schéma nonlinéaire pour l'approximation numérique d'un système hyperbolique non conservatif. *C. R., Math., Acad. Sci. Paris*, 335(12):1069–1072.

[3] Berthon C. and Coquel F. (2002), Nonlinear projection methods for multi-entropies Navier-Stokes systems. In *Hafez, M. M. (ed.) et al., Innovative methods for numerical solutions of partial differential equations. Proceedings of the symposium on progress in numerical solutions of partial differential equations, Arcachon, France, July 11-13, 1998. In honor of Phil Roe on the occasion of his 60th birthday.* , pages 278–304. Singapore: World Scientific..

[4] Berthon C. and Coquel F., (1999), Travelling wave solutions of a convective diffusive system with first and second order terms in nonconservation form. *Hyperbolic problems: theory, numerics, applications, Vol. I*, Internat. Ser. Numer. Math., 129, Birkhäuser, Basel, 47–54.

[5] Berthon C. and Reignier R., (2003), An approximate nonlinear projection scheme for a combustion model. *M2AN*, 37(3):451–478.

[6] Chalons C., (2002), *Bilans d'entropie discrets dans l'approximation numérique des chocs non classiques. Application aux équations de Navier-Stokes multi-pression 2D et à quelques systèmes visco-capillaires.* PhD Thesis, Ecole polytechnique (Paris, France).

[7] Chern I-L., Glimm J., McBryan O., Plohr B., and Yaniv S., (1986), Front tracking for gas dynamics. *J. Comput. Phys.*, 62:83–110.

[8] Dal Maso G., LeFloch P., Murat F., (1995), Definition and weak stability of a non conservative product. *J. Math. Pures Appl.*, 74:483–548.

[9] Declercq E., Forestier A., Hérard J.-M., Louis X., Poissant G., (2000), An exact Riemann solver for multicomponent turbulent flow. *Int. J. Comput. Fluid Dyn.*, 14(2):117–131.

[10] Declercq E., Forestier A., Hérard J.-M., Louis X., Poissant G., (2003), Comparison of numerical solvers for a multicomponent turbulent flow. II. *Int. J. Comput. Fluid Dyn.*, 17(3):169–182, 2003.

[11] Drew D. and Passman S., (1998), *Theory of multicomponent fluids*, volume 135 of *Applied Mathematical Sciences*. Springer.

[12] Forestier A., Hérard J.-M., Louis X., (1997), Solveur de type Godunov pour simuler les écoulements turbulents compressibles. *C. R., Math., Acad. Sci. Paris*, 324(8):919–926, 1997.

[13] Glimm J., Grove J.W., Xiao Lin L., Shyue K.-M., and Zeng Y., (1998), Three-dimensional front tracking. *SIAM J. Sci. Comput.*, 19(3):703–727.

[14] Glimm J., Isaacson E., Marchesin D., and McBryan O., (1981), Front tracking for hyperbolic systems. *Adv. Appl. Math.*, 2:91–119.

[15] Godlewski E. and Raviart P.A., (1996), *Numerical approximation of hyperbilic systems of conservation law.* J.E. Marsden and L. Sirovich: Springer-Verlag New Yorc, Inc., second edition.

[16] Lagoutière F., (2000), *Modélisation mathématique et résolution numérique de problèmes de fluides compressibles à plusieurs constituants*. PhD Thesis, Université Paris VI.

[17] Louis X., (1995), *Modélisation numérique de la turbulence compressible.* PhD Thesis, Université Paris VI.

[18] Massoni J., Saurel R., Nkonga B., and Abgrall R., (2001), Proposition de methodes et modeles euleriens pour les problemes a interfaces entre fluides compressibles en presence de transfert de chaleur. *Journal of Heat and Mass Transfer*, 45(6):1287–1307.

[19] Mohammadi B. and Pironneau O., (1994), *Analysis of the K-Epsilon Turbulence Model*. Research in Applied Mathematics. Masson Eds.

[20] Nkonga B., (2000), On the conservative and accurate CFD approximations for moving meshes and moving boundaries. *Comput. Methods Appl. Mech. Engrg*, 190:1801–1825.

[21] Partom I.S., (1987), Application of the VOF method to the sloshing of a fluid in a partially filled cylindrical container. *Int. J. Numer. Methods Fluids*, 7:535–550.

[22] Raviart P.-A. and Sainsaulieu L., (1995), A nonconservative hyperbolic system modeling spray dynamics. I: Solution of the Riemann problem. *Math. Models Methods Appl. Sci.*, 5(3):297–333.

[23] Saurel R. and Abgrall R., (1999), A multiphase Godunov method for compressible multifluid and multiphase flows. *J. Comput. Phys.*, 150(2):425–467.

[24] Saurel R. and Abgrall R., (1999), A simple method for compressible multifluid flows. *Siam J. Sci. Comp.*, 21(3):1115–1145.

[25] Shyue K.-M., (1998), An efficient shock-capturing algorithm for compressible multicomponent problems. *J. Comp. Phys.*, 1:208–242.

[26] Zhao Y., Tan H.H., and Zhang B., (2002), A high-resolution characteristics-based implicit dual time-stepping VOF method for free surface flow simulation on unstructured grids. *J. Comput. Phys.*, 183(1):233–273.

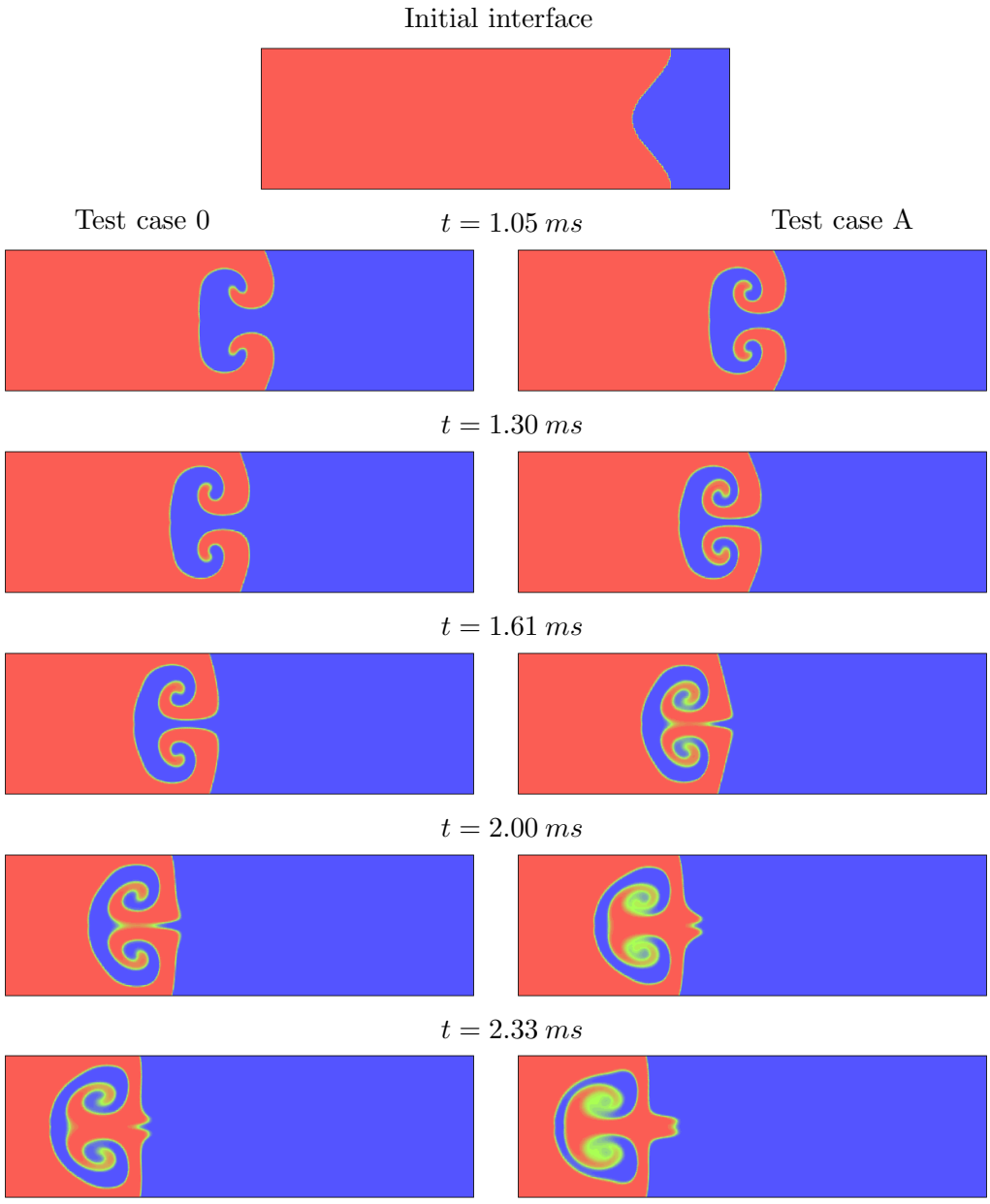

Figure 3: Influence of the fluctuations on the behavior of the Richtmeyer-Meshkov instability. Time evolution of a color function solution with (right) and without (left) an initial fluctuating zone around the material interface. Profiles (defined by the same color function) at the times $t = 0$, $t = 1.05\,ms$, $t = 1.3\,ms$, $t = 1.61\,ms$, $t = 2.0\,ms$, $t = 2.33\,ms$.

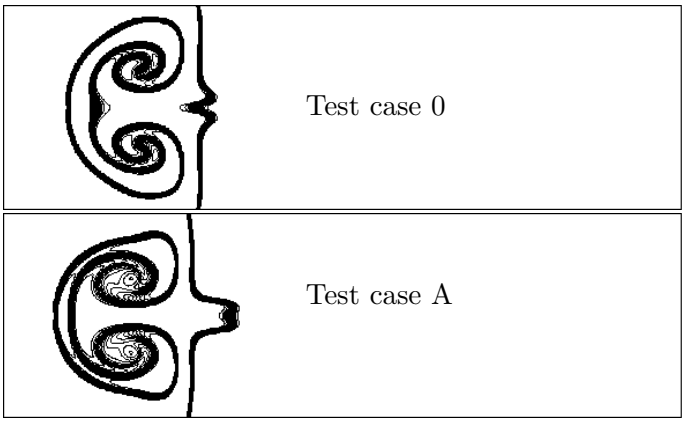

Figure 4: Comparison of the numerical material interface profiles (defined by the same color function), at the time $t = 2.33\,ms$, between computations performed without (Test case 0) and with (Test case A) an initial fluctuating zone around the material interface.

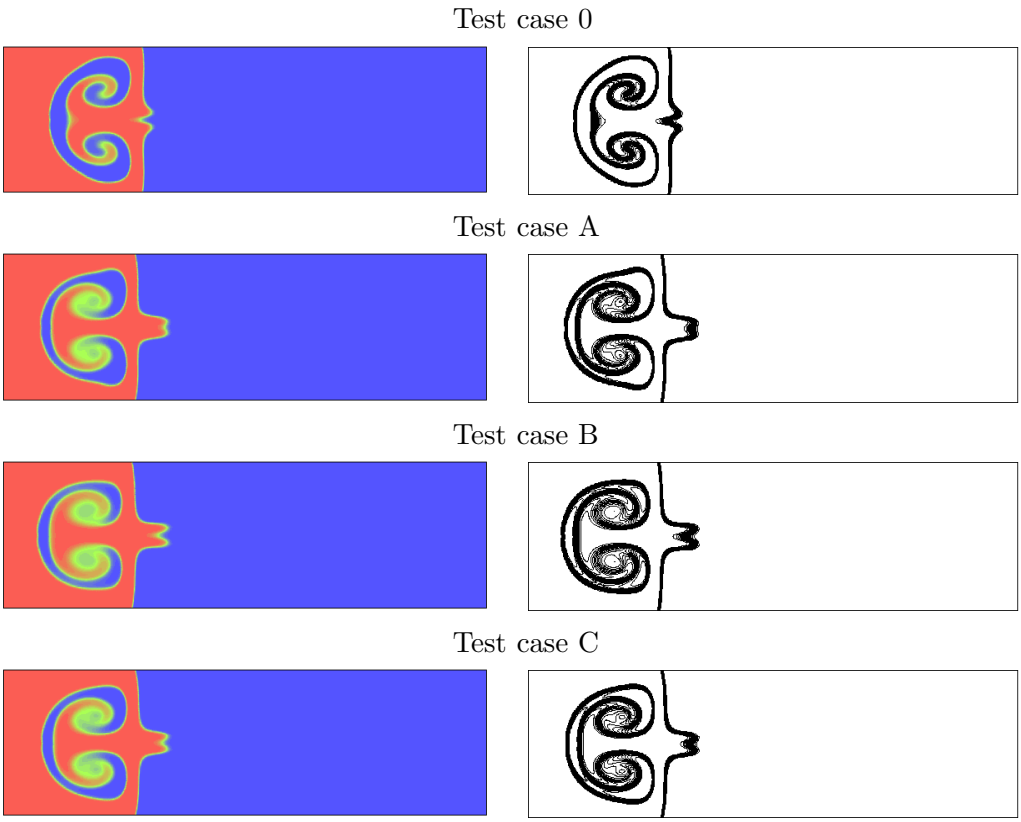

Figure 5: Effects of the initial fluctuating conditions on the Richtmeyer-Meshkov instability. Profiles (defined by the same color function) at the time $t = 2.33\,ms$.

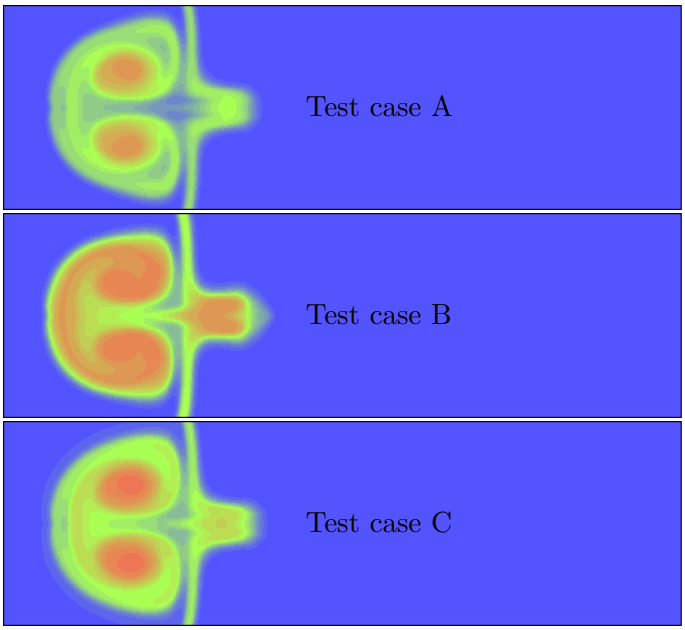

Figure 6: Fluctuating kinetic energy ρk at time $t = 2.33\,ms$. Profiles for the test cases A, B and C